

Multi-spectral photo-acoustic molecular tomography resolves fluorochrome distribution with high resolution and sensitivity in small animals

Daniel Razansky^{1,3,*}, Claudio Vinegoni^{1,2}, and Vasilis Ntziachristos^{1,3}

¹Laboratory for Bio-optics and Molecular Imaging, Center for Molecular Imaging Research, Massachusetts General Hospital and Harvard Medical School, Charlestown, MA 02129

²Center for System Biology, Massachusetts General Hospital and Harvard Medical School, 185 Cambridge Street, Boston, MA, 02114, USA.

³Institute for Biological and Medical Imaging, Technical University of Munich and Helmholtz Center Munich, Ingolstädter Landstraße 1, 85764 Neuherberg, Germany.

ABSTRACT

Current non-invasive imaging methods of fluorescent molecular probes in the visible and near-infrared suffer from low spatial resolution as a result of rapid light diffusion in biological tissues. We show that three-dimensional distribution of fluorochromes deep in small animals can be resolved with below 25 femtomole sensitivity and 150 microns spatial resolution by means of multi-spectral photoacoustic molecular tomography. The low sensitivity limit of the method is enabled by using the highly resonant absorption spectrum of a commonly used near-infrared fluorescent molecular probe Alexa Fluor® 750 in order to acquire differential images at multiple wavelengths with tomographic topology suitable for whole-body small animal imaging.

I. INTRODUCTION

The use of fluorescence in the visible and near-infrared spectra for visualizing functional and molecular activity *in-vivo* offers the greatest selection of contrast and probing mechanisms [1], [2], as compared to less molecular-specific imaging modalities, such as magnetic resonance imaging, ultrasound, ionizing-radiation-based methods etc. During the last decade, a lot of efforts were applied into developing highly sensitive and specific fluorescent molecular beacons for *in-vivo* optical imaging. A large number of commercially available fluorescent probes are currently offered, from non-specific fluorescent dyes to targeted or activable photoproteins and fluorogenic-substrate-sensitive fluorochromes [3]. So far, fluorescent contrast was proven efficient in a number of clinical and small-animal applications, including gene expression profiling, detecting protease up-regulation associated with cancer growth and inflammation, continuous monitoring of the efficacy of anti-cancer treatments and other therapeutic drugs [4]-[8].

Optical probing of molecular function and gene expression may indeed offer a powerful molecular imaging tool, however, its *in-vivo* depth-resolved imaging is hindered by highly diffusive nature of biological tissues. Therefore, fluorescence-sensitive micron-scale-resolution optical imaging methods, like multiphoton, epifluorescence or confocal microscopies, become inefficient when trying to image at depths beyond one mean free path of photons in tissue, which is on the order of 0.5 mm in most tissues [9]. Whole-body imaging of three-dimensional fluorochrome distributions in small animals has recently become possible with introduction of fluorescence molecular tomography (FMT) [10]-[11]. FMT utilizes point illumination and detection of light intensity at the surface of optically diffusive object. The light diffusion equation, used as a forward model of light propagation in FMT, has been proved adequate when the light sources and detectors are separated by more than few mean free path lengths in turbid tissues [12], fitting well small animal dimensions. Nevertheless, both spatial resolution and accuracy of optical-diffusion-based imaging methods are compromised by diffusion path length as well as highly heterogeneous nature of optical absorption and diffusion in realistic tissues.

* Electronic mail: daniel.razansky@helmholtz-muenchen.de

Recently, tomographic imaging of tissues using photoacoustics, has demonstrated high-resolution capabilities both clinically and in small animals with penetration depths varying from several millimeters [13] up to centimeters range, when dealing with relatively low absorption media, such as chicken or human breast tissue [14]. Photoacoustic imaging relies on ultrasonic detection of photoacoustically-induced signals following absorption of pulsed light [15]. The amplitude of the generated broadband ultrasound waves reflects local optical absorption properties of tissue. Since scattering of ultrasonic waves in biological tissues is extremely weak, as compared to that of light, biomedical photoacoustic imaging combines high optical absorption contrast with diffraction limited resolution of ultrasonic imaging. It was proven efficient in imaging vascular trees, blood oxygenation monitoring, tumor angiogenesis, as well as sensitive to some contrast agents, like exogenous chromophores, light-absorbing nanoparticles, and chromogenic assays [13]-[18].

In this study, we resolve three-dimensional fluorescence distribution deep in small animals, with both high spatial resolution and sensitivity, using multi-spectral photoacoustic molecular tomography. Multi-spectral methods have been shown useful in imaging fluorochrome distributions in tissues by pure optical methods [12]. In photoacoustics, they were applied for resolving tissue chromophore concentrations [17], as well as for detection of optical dyes in non-absorbing phantoms [19]. Imaging fluorochrome distributions in real tissues by means of photoacoustics presents several challenges. First, *in-vivo* optical absorption contrast can reach up to two orders of magnitude at some wavelengths [9]. In particular, some areas with high blood content are very absorptive, making the fluorochrome hard to distinguish from the highly absorbing background. Additionally, some tissue chromophores, e.g. oxy-hemoglobin, may considerably change their optical absorption with the wavelength, especially in the visible. This might complicate their detection even when using multi-spectral methods. Some factors, however, act in favor of using photoacoustics for detecting fluorescence *in-vivo*. Most of the commonly-utilized exogenous as well as endogenous fluorochromes exhibit highly resonant optical absorption spectra in the vicinity of their peak excitation wavelength. The imaging can be facilitated by acquiring photoacoustic images at several adjacent wavelengths on the steep resonant slope of fluorochrome absorption spectra. Since optical absorption of most tissue structures present much smoother wavelength dependence, especially in the near-infrared [9], an intrinsic tissue contrast can be readily suppressed and highly sensitive imaging of fluorochrome distribution in tissue obtained by subtracting photoacoustic images at several different but close wavelengths.

II. METHODS

The experimental setup for our photoacoustic measurements is shown in Fig. 1. A tunable OPO laser (Vibrant-532-I, Opotek Inc., Carlsbad, CA) pumped with Q-switched Nd:YAG laser produced 10 ns duration pulses in the near-infrared (680-950nm) with repetition frequency of 20 Hz. Its output fluence was kept below 20mJ/cm² per pulse as to meet pulsed laser safety criteria [20]. A cylindrically-focused broadband ultrasonic transducer (Model V382, Panametrics) with central frequency of 3.7 Mhz and 75% bandwidth was used to record the photoacoustic signals transmitted from the imaged object, which was rotated 360° with 2° steps. The time-resolved signals, recorded by the transducer were amplified, digitized, and averaged by an embedded oscilloscope PCI card at 100 Msp/s (NI PCI-5122, National Instruments Corp., Austin, TX) and 14-bits vertical resolution. The rotation and translation stages were controlled via stage controller (ESP-3000, Newport Corp., Irvine, CA). The laser, stage controller and data acquisition were all synchronized via PC-based Labview 7.0 program (National Instruments Corp., Austin, TX). The total acquisition time per two-dimensional image slice was 5 min.

For our multispectral experiments, we used AF750 (Alexa Fluor® 750, Invitrogen Corp., Carlsbad, CA), a near-infrared fluorescent dye, having multiple well-established and commercially available molecular probing and cell targeting capabilities [5], [21]. The wavelength dependence of its molar extinction coefficient is depicted in Fig. 2 along with the corresponding data for several tissue chromophores. The molar extinction of AF750 peaks at 240,000 M⁻¹cm⁻¹ for 750 nm, which greatly exceeds that of most chromophores in the near-infrared (Fig. 2). Another favorable feature of AF750 is its relatively low 0.12 quantum yield, leaving more energy for producing the photoacoustic signal and less for fluorescence energy transfer. Fig. 2 also demonstrates the very broadband absorption behavior of some chromophores as compared to highly resonant (narrowband) behavior of fluorescence dye, making it a good candidate for our multi-spectral separation method. It is also expected that the method will provide good results for AF750 even in the presence of whole blood, whose optical absorption is gradually increasing with the wavelength above 750 nm, while the absorption of AF750 is rapidly decreasing by more than two orders of magnitude within 60 nm following 750 nm (Fig. 2).

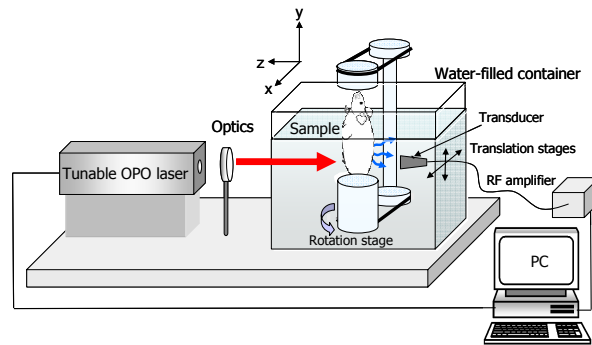


Fig. 1. Experimental setup for multispectral photoacoustic molecular tomography.

We have chosen a pelvic limb of a wild-type mouse in the interosseous space of crus area as our imaging target with elliptic-like cross-section of about 10 mm by 7 mm in size in the imaging plane. It was selected not only for the demonstration purposes but also because it happens to be quite difficult to perform three-dimensional (depth-resolved) FMT imaging in this area due to its irregular conical shape and relatively small dimensions, both severely restricting the field-of-view of FMT source and detector patterns. It might also present several challenges for photoacoustic imaging due to extensive vascularization and presence of acoustically mismatched impedance of the bones. Yet, the importance of the ability to visualize proximities in small animal fluorescence-based molecular imaging research was previously demonstrated [22].

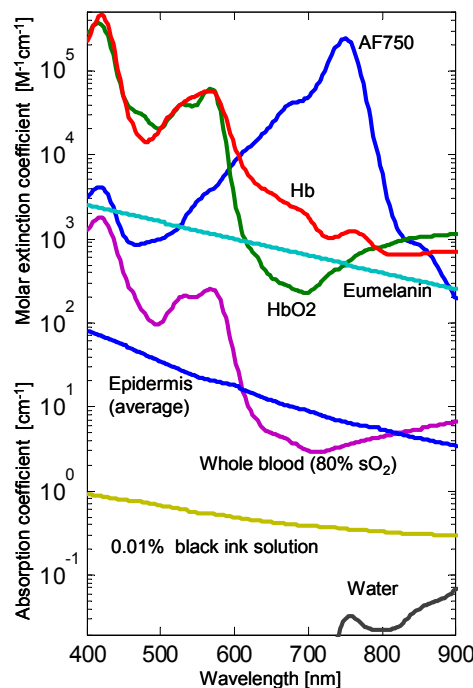


Fig. 2. Wavelength dependence of absorption by AF750 and different chromophores and tissues.

The imaging sessions were performed immediately after injecting solution containing 250 pmol of AF750 into the imaged area. The photoacoustic tomographic data was acquired at three different wavelengths, namely, 750 nm, 770 nm, and 790 nm, selected among larger available pool of wavelengths for demonstration purposes. Tomographic inversion was performed separately for each acquired wavelength using filtered backprojection [13]. The image reconstruction on dual-core Pentium IV 3.2 Ghz processor, having 2GB RAM, typically required 2 sec per two-dimensional image slice using 256 x 256 mesh. In contrast to inversions applied assuming homogenous light distribution within appropriately selected sections of tissue [13], [17], [18], [10], the particular inversion scheme, applied here for whole-body imaging, incorporates a diffusive model of photon propagation in tissues, in order to correct the raw RF data acquired for the intensity drop of the signal due to the light attenuation as a function of propagation distance. To achieve this, average known optical absorption and scattering coefficients at the applied wavelengths [9] were utilized. The imaging accuracy achieved with this approach was satisfactory, but iterative solutions using photo-acoustic data have been recently investigated and could further improve image quality [23]. Subsequently, the multi-spectral processing applied, fitted for the known absorption spectrum of the fluorochrome employed to the reconstructed absorption value at each pixel of the images at the different wavelengths. The resulting image therefore reports on the intensity of the fitted curve, on a per-pixel basis.

III. RESULTS

The reconstructed photoacoustic images are presented in Figs. 3(a)-(c) along with the corresponding ultrasonic image, acquired approximately at the same imaging plane, by VisualSonics Vevo 660TM (VisualSonics Inc., Toronto, Ontario) 25 Mhz high-resolution ultrasound imaging system. The triangular-shape *tibia* as well as the *fibula* bones are clearly visualized in both photoacoustic and ultrasonically-acquired images. It should be noted that, as expected, little difference exists between the three photoacoustic images due to small wavelength shifts. Also, the presence of the fluorescence dye cannot be clearly distinguished by just inspecting the images since optical absorption of various tissue structures in the image varies greatly (e.g. between bones and other highly vascularized tissue structures), thus increasing the dynamic range of the images.

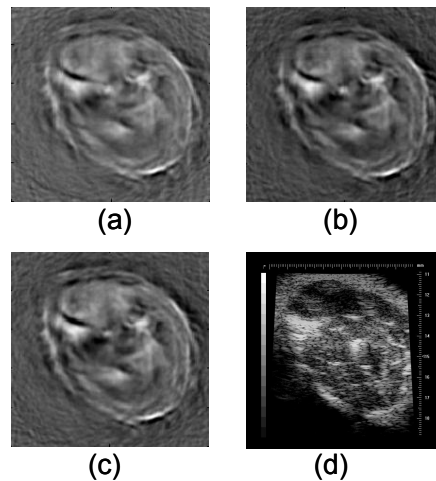


Fig. 3. Photoacoustic tomography images, acquired at (a) 750nm; (b) 770 nm; and (c) 790 nm illumination; as compared to (d) ultrasound image acquired at 25Mhz.

However, when making the differential images between the different wavelengths (Figs. 4(c)-(f)), the tissue contrast is readily suppressed, giving rise to the highly resonant contrast of AF750 dye, which can clearly be distinguished from the background tissue absorption. When comparing Figs. 4(c) and (e) to Figs. 4(d) and (f), one notes that the presence of AF750 is more prominent for the images representing the difference between 790 nm and 750 nm. This is due to the fact that AF750 still has a residual absorption of around 50% at 770 nm, as compared to negligible absorption at 790 nm, thus

the contrast of AF750 between 790 nm and 750 nm is indeed expected to be greater than the one between 770 nm and 750 nm. We have also prepared a planar fluorescence image of the sliced tissue at approximately the same imaging plane to confirm the presence of AF750 (Fig. 4(b)). Indeed, the freezing and slicing process might greatly disturb tissue composition and shape as well as cannot accurately represent the imaged plane, however, the overall location of the fluorescence in Fig. 4(b) coincides well with the multispectral images.

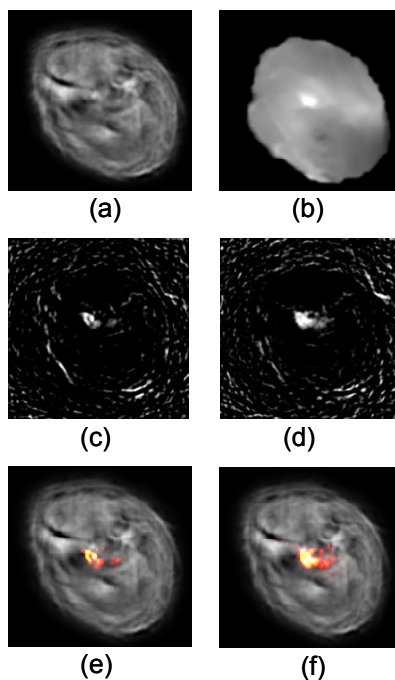


Fig. 4. Multispectral photoacoustic tomography images: (a) Regular photoacoustic image at 750 nm; (b) Planar fluorescence image of the sliced tissue; (c) Differential photoacoustic image between 770 nm and 790 nm images; (d) Differential photoacoustic image between 750 nm and 790 nm; (e) and (f) are the corresponding differential images superimposed onto the regular image at 750 nm.

We have calculated the contrast to noise ratio of our images to be above 11 per given measurement parameters. The maximal lateral resolution in the x-z plane (Fig. 1) is limited by the 5Mhz (-6db) bandwidth of the transducer to be on the order of 150 μm , while the vertical resolution is limited by the focal width of the cylindrically-focused transducer to approximately 1.2 mm at 3.7 Mhz. To estimate the sensitivity limit of our system, one may thus take the resolution limited voxel of our system to be $0.15 \times 0.15 \times 1.2 \text{ mm} = 0.027 \text{ mm}^3$. Considering the total volume of the injected AF750 solution (25 μl), the resulting lowest resolvable amount of the fluorescent dye in such a voxel was below 25 femtomoles, amount comparable to the current state-of-the-art FMT systems [4]-[8], [10]-[12]. Note, that this worst-case scenario assumes that the whole volume of the injected solution remained at one place immediately after the injection and has not degraded or diffused out during the imaging sessions.

IV. DISCUSSION AND CONCLUSIONS

Given the great availability and selection of fluorochromes, their probing and targeting mechanisms, the herein presented multi-spectral photoacoustic tomography method holds a great promise of becoming a valuable molecular imaging tool. As compared to most pure chromophores, having relatively broadband optical absorption characteristics, many fluorochromes exhibit sharp resonances in the vicinity of their peak excitation spectra, making them convenient candidates for highly sensitive multi-spectral photoacoustic imaging. Also, some fluorochromes, especially in the near-infrared, possess relative high molar extinction coefficients in excess of $10^5 \text{ M}^{-1}\text{cm}^{-1}$ in conjunction with low quantum yield (acting in favor of photoacoustic signal generation). Thus, they might possibly be distinguished by the

multispectral photoacoustic imaging at reasonable concentrations even in the presence of highly absorbing tissue chromophores.

In this study, we resolve three-dimensional fluorescence distribution deep in wild-type Balb/c mice using multi-spectral photoacoustic molecular tomography. The low sensitivity limit of the method is enabled by using the highly resonant absorption spectrum of a commonly used near-infrared fluorescent molecular probe (Alexa Fluor® 750) in order to acquire photoacoustic images at multiple wavelengths with tomographic topology suitable for whole-body small animal imaging. Since optical absorption of most tissue structures presents much smoother wavelength dependence, especially in the near-infrared, an intrinsic tissue contrast is readily suppressed and highly sensitive imaging of fluorochrome distribution in tissue obtained by spectral matching. As opposed to most previous photoacoustic studies, assuming planar illumination and nearly homogenous light distribution within appropriately selected sections of tissue, we have applied an imaging configuration suitable for whole-body small animal imaging applications and presented imaging results for photoacoustically-challenging portion of mouse body, having relatively high optical absorption contrasts and high degrees of both optical and acoustic heterogeneities. We have measured the sensitivity limit for resolving AF750 in the current experiment to be below 25 fmol with spatial imaging resolution on the order of 150 μm . However, both resolution and sensitivity will greatly depend on the particular experimental setup, dimensions and properties of the imaged object. The average depth of the fluorochromes in the current study was between 3.5 and 5 mm below the skin surface. In general, increasing imaging depth will increase the minimal detectable limits. It worth noting, however, that the detection limits will be deteriorating much slower as a function of depth in the photoacoustic case as compared to diffusion optics since, for the latter, the information is affected by light diffusion and absorption both ways (towards the target and on its way back), while the former suffers from light-related effects only on its way towards the target. Naturally, detection limits and/or spatial resolution of our method can also be improved by e.g. increasing transducer's sensitivity and/or bandwidth, improving the illumination strategy, or increasing signal averaging. Finally, introducing ultrasonic detection arrays in photoacoustic measurements [19], might turn the proposed method into a powerful real-time molecular imaging modality. The suggested method thus holds a promise of significantly enhancing our ability to visualize both functional and molecular information in-vivo.

REFERENCES

- [1] R. Weissleder, "Molecular imaging in cancer," *Science*, 312, pp. 1168-1171, (2006).
- [2] V. Ntziachristos, J. Ripoll, L.V. Wang and R. Weissleder, "Looking and listening to light: the evolution of whole-body photonic imaging," *Nature Biotechnology*, vol. 23, 313-320, (2005).
- [3] B. N. Giepmans, S.R. Adams, M.H. Ellisman, and R.Y. Tsien, "The fluorescent toolbox for assessing protein location and function," *Science* vol. 312, pp. 217-224, (2006).
- [4] V. Ntziachristos, E. A. Schellenberger, J. Ripoll, D. Yessayan, E. Graves, A. Bogdanov Jr., L. Josephson, and R. Weissleder, "Visualization of antitumor treatment by means of fluorescence molecular tomography with an annexin V-Cy5.5 conjugate", *Proc. Natl. Acad. Sci.* 101, 12294-12299 (2004).
- [5] X. Montet, V. Ntziachristos, J. Grimm, and R. Weissleder, "Tomographic fluorescence mapping of tumor target", *Cancer Res.* 65, 6330-6336 (2005).
- [6] V. Ntziachristos, C.-H. Tung, C. Bremer, and R. Weissleder, "Fluorescence molecular tomography resolves protease activity in vivo", *Nature Med.* 8, 757-760 (2002).
- [7] D. E. Sosnovik, M. Nahrendorf, N. Deliolanis, M. Novikov, E. Aikawa, L. Josephson, A. Rosenzweig, R. Weissleder, and V. Ntziachristos, "Fluorescence tomography and magnetic resonance imaging of myocardial macrophage infiltration in infarcted myocardium in vivo", *Circulation* 115, 1384-1391 (2007).
- [8] J. Grimm, D. G. Kirsch, S. D. Windsor, C. F. Bender Kim, P. M. Santiago, V. Ntziachristos, T. Jacks, and R. Weissleder, "Use of gene expression profiling to direct in vivo molecular imaging of lung cancer", *Proc. Natl. Acad. Sci.* 102, 14404-14409 (2005).
- [9] A. J. Welch and M. J. C. van Gemert, Editors, "Optical thermal response of laser-irradiated tissue", Plenum Press, New-York, 1995.
- [10] E. E. Graves, J. Ripoll, R. Weissleder, and V. Ntziachristos, "A submillimeter resolution fluorescence molecular imaging system for small animal imaging", *Med. Phys.* 21, 492-500 (2004).
- [11] N. Deliolanis, T. Lesser, D. Hyde, A. Soubret, J. Ripoll, and V. Ntziachristos, "Free-space fluorescence molecular tomography utilizing 360° geometry projections", *Opt. Lett.* 32, 382-384 (2007).

- [12] V. Ntziachristos and R. Weissleder, "Experimental three-dimensional fluorescence reconstruction of diffuse media by use of a normalized Born approximation", *Opt. Lett.* 26, 893-895 (2001).
- [13] H. F. Zhang, K. Maslov, G. Stoica, and L. V. Wang, "Functional photoacoustic microscopy for high resolution and noninvasive *in-vivo* imaging", *Nature Biotechnology*, 24(7), pp. 848-851, (2006).
- [14] R. O. Esenaliev, A. A. Karabutov, and A. A. Oraevsky, "Sensitivity of laser opto-acoustic imaging in detection of small deeply embedded tumors", *IEEE J. Sel. Topics Quantum Electron.*, 5(4), pp. 981-988, 1999.
- [15] L. V. Wang, "Ultrasound-mediated biophotonic imaging: A review of acousto-optical tomography and photoacoustic tomography", *Disease Markers* 19, 123-138 (2003-2004).
- [16] R. I Siphanto et al., "Serial noninvasive photoacoustic imaging of neurovascularization in tumor angiogenesis", *Optics Express*, 13(1), pp. 89-95, (2005).
- [17] J. Laufer, D. Delpy, C. Elwell and P. Beard, "Quantitative spatially resolved measurement of tissue chromophore concentrations using photoacoustic spectroscopy: application to the measurement of blood oxygenation and haemoglobin concentration", *Phys. Med. Biol.*, 52, pp. 41-68, (2007).
- [18] L. Li, R. J. Zemp, G. Lungu, G. Stoica, and L. V. Wang, "Photoacoustic imaging of lacZ gene expression in vivo", *JBO Letters*, 12(2), 020504, (2007).
- [19] R. A. Kruger, W. L. Kiser Jr., D. R. Reinecke, G. A. Kruger, and K. D. Miller, "Thermoacoustic optical molecular imaging of small animals", *Mol. Imag.* 2, 113-123 (2003).
- [20] American National Standards Institute, American National Standard for the Safe Use of Lasers in Health Care Facilities: Standard Z136.1-2000_ANSI, Inc., New York, 2000.
- [21] C. Bremer, V. Ntziachristos, and R. Weissleder, "Optical-based molecular imaging: contrast agents and potential medical applications", *European Radiology*, 13(2), pp. 231-243, (2003).
- [22] W. T. Chen et al., "Arthritis imaging using a near-infrared fluorescence folate-targeted probe", *Arthritis Research and Therapy*, 7 (2), pp. R310-R317, (2005).
- [23] Z. Yuan and H. B. Jiang, "Three-dimensional finite-element-based photoacoustic tomography: Reconstruction algorithm and simulations", *Med. Phys.* 34, 538-546 (2007).